Numerical simulation of the non-Newtonian mixing layer

By J. Azaiez [1] AND G. M. Homsy [1]

1. Motivation and objectives

The problem of transition from laminar to turbulent flow in free shear layers is of great practical interest. Many natural and industrial situations involve a free shear flow, and it is very crucial to understand the mechanisms governing the process of transition to turbulence in order to predict and, if possible, control the evolution of the flow. Much past work related to the instability of the mixing layer has dealt exclusively with Newtonian fluids. The interaction between the large scale two-dimensional structures, namely the roll-up and the pairing, and vortex stretching has been explored extensively, leading to a better understanding of the mechanisms of transition to turbulence.

In a wide range of applications, the reduction of hydrodynamic drag is of great importance for reasons of economy and performance. Delaying or accelerating laminar-to-turbulent transition of a free shear layer has many obvious advantages. To delay transition to turbulence as far downstream as possible allows a gain in energy efficiency in some industrial processes. Accelerating the transition, on the other hand, can be of interest in processes where high mixing is desired.

Among the modern techniques for drag reduction are riblets, large-scale eddy breakup devices, and flow suction. Another avenue for drag reduction is the use of polymer additives in the flow. The study of drag reduction obtained by the addition of small amounts of high polymers has been an active area of research for the last three decades (see Sellin and Moses 1989).

This work is a continuing effort to advance our understanding of the effects of polymer additives on the structures of the mixing layer. In anticipation of full non-linear simulations of the non-Newtonian mixing layer, we examined in a first stage the linear stability of the non-Newtonian mixing layer (Azaiez and Homsy 1992). The results of this study show that, for a fluid described by the Oldroyd-B model, viscoelasticity reduces the instability of the inviscid mixing layer in a special limit where the ratio $(\frac{We}{Re})$ is of order 1 where We is the Weissenberg number, a measure of the elasticity of the flow, and Re is the Reynolds number.

In the present study, we will pursue this project with numerical simulations of the non-Newtonian mixing layer. Our primary objective is to determine the effects of viscoelasticity on the roll-up structure. We will also examine the origin of the numerical instabilities usually encountered in the simulations of non-Newtonian fluids.

1 Stanford University

2. Accomplishments

2.1 Problem Definition

We used a vorticity-streamfunction formulation for Cauchy's momentum equation. This equation is closed through evolution equations relating the stress tensor to the shear rate tensor. In all the subsequent analysis, the stress tensor is written as the sum of two stresses:

$$\tau = \tau^s + \tau^p \tag{1}$$

In Eq. (1), the first term corresponds to the contribution of the Newtonian solvent and is proportional to the shear rate tensor:

$$\tau^s \equiv \eta_s \dot{\gamma} \tag{2}$$

where η_s is the solvent viscosity. The second term represents the polymeric contribution:

$$\tau^p \equiv \eta_p a \tag{3}$$

where η_p is the polymeric contribution to the shear viscosity and a is the tensor related to the polymeric stress. Equations for $a(x, y, t)$ define a rheological model and must be given to close the equations. We let $\kappa = \dfrac{\eta_s}{\eta_s + \eta_p} = \dfrac{\eta_s}{\eta}$ be the ratio of viscosities. We fix $\kappa = 0.5$ in all the simulations.

The first step in studying the non-Newtonian behavior of a given flow is the choice of the appropriate constitutive equation required to describe the physics of the non-Newtonian fluid. In the present study, we will focus on two rheological models known to describe dilute polymer solutions: The popular Oldroyd-B model and the FENE model.

We are initially interested in the roll-up of the shear layer into spanwise vortices. The initial base state for the numerical simulations is given by a hyperbolic tangent velocity profile on which we superposed a *cos* perturbation on the stream function with the maximum at the centerline $y = 0$. The most unstable wave number, $\alpha = 0.44$, has been used in all the simulations. The extension of the domain in the streamwise direction is set to $\dfrac{2\pi}{\alpha}\delta$ with δ the momentum thickness of the mixing layer. The vertical extension has been heuristically fixed equal to 8δ. The Reynolds number is defined as $Re = \dfrac{\delta u_0}{\eta}$ where $u_0 = (U_1 - U_2)/2$. U_1 and U_2 are the free-stream velocities.

The vorticity equation and the rheological equations lead to a system of partial differential equations that we solve by a pseudo-spectral method based on the Hartley transform. We use a fourth order Runge-Kutta method to advance the equations for the Hartley coefficients in time.

2.2 The Oldroyd-B model

The Oldroyd-B model describes well the behavior of polymeric liquids composed of a low concentration of high molecular weight polymer in a very viscous Newtonian

solvent at moderate shear rates. These fluids have come to be known as Boger fluids. Data on well-characterized Boger fluids are available (Boger 1977; Mackay & Boger 1987), allowing a comparison of theoretical predictions with experimental results. The Oldroyd-B rheological equations can be derived from a molecular model in which the polymer molecule is idealized as a Hookean spring connecting two Brownian beads (Bird *et al.* 1987).

As above, the stress tensor τ can be written as the sum of two stresses:

$$\tau = \tau^s + \tau^p = \eta[\kappa\dot{\gamma} + (1-\kappa)a]$$

The tensor a satisfies the upper convected Maxwell equation:

$$a_{ij} + \lambda\frac{\delta a_{ij}}{\delta t} = \dot{\gamma}_{ij} \tag{4}$$

where:

$$\frac{\delta a_{ij}}{\delta t} = \frac{\partial a}{\partial t} + \vec{v}\cdot\nabla a - \nabla\vec{v}^{\perp}\cdot a - a\cdot\nabla\vec{v} \tag{5}$$

is the upper-convected derivative of a, and λ is the polymer relaxation time. Using u_o and δ as the reference velocity and the reference length, respectively, Eq. (4) is characterized by one dimensionless group: the Weissenberg number, $We = \frac{\lambda u_o}{\delta}$, a dimensionless measure of the elasticity of the flow. The Oldroyd-B model contains both the upper-convected Maxwell fluid ($\eta_s = 0 \Leftrightarrow \kappa = 0$) and the Newtonian fluid ($\eta_p = 0 \Leftrightarrow \kappa = 1$).

For small values of the Weissenberg number, We, the flow does not show any changes from the Newtonian case. Obviously, viscoelastic terms are not large enough to affect the inertial mechanisms.

As we increase the Weissenberg number, the code starts to develop instabilities and ceases to converge before the completion of the roll-up. Similar problems related to the complexity of the coupling between viscoelastic and inertia effects have been reported by Joseph *et al.* (1985) and Crochet and Delvaux (1990). Numerical instabilities in the simulations of viscoelastic fluids have in fact been the subject of many studies. These studies have in general focused on the Maxwell model, a special case of the Oldroyd-B model, and showed that the absence of the diffusive term in the vorticity equation may be the reason for the blow-up of the numerical schemes. Other studies attribute the breakup of the numerical codes to the reaching of a supercritical regime where the vorticity equation becomes hyperbolic (Joseph (1990)). This regime is reached whenever the viscoelastic Mach number $M = (We\ Re)^{1/2}$ exceeds one. (Crochet and Delvaux (1990))

In the present study, we shall show that the divergence of codes using the Oldroyd-B model is attributed to a relaxation term in the stress equations which plays a major role in the development and growth of the instability. Writing Eq. (5) in component form, we have:

$$\frac{\partial a_{12}}{\partial t} = \underbrace{-\frac{a_{12}}{We}}_{\textit{Damping Term}} \underbrace{-[u\frac{\partial}{\partial x} + v\frac{\partial}{\partial y}]a_{12}}_{\textit{Convective Term}} + \underbrace{\frac{(\partial_{y^2} - \partial_{x^2})\psi}{We} - a_{11}\frac{\partial^2\psi}{\partial x^2} + a_{22}\frac{\partial^2\psi}{\partial x^2}}$$

$$\frac{\partial a_{11}}{\partial t} = \underbrace{\underbrace{[-\frac{1}{We} + 2\frac{\partial^2 \psi}{\partial x \partial y}]}_{1^{st}\ relaxation\ coeff.}}_{Damping\ Term} a_{11} - \underbrace{[u\frac{\partial}{\partial x} + v\frac{\partial}{\partial y}]a_{11}}_{Convective\ Term} + \underbrace{2(\frac{\partial^2{}_{xy}\psi}{We} + a_{12}\frac{\partial^2 \psi}{\partial y^2})}$$

$$\frac{\partial a_{22}}{\partial t} = \underbrace{\underbrace{-[\frac{1}{We} + 2\frac{\partial^2 \psi}{\partial x \partial y}]}_{2^{nd}\ Relaxation\ Coeff.}}_{Damping\ Term} a_{22} - \underbrace{[u\frac{\partial}{\partial x} + v\frac{\partial}{\partial y}]a_{22}}_{Convective\ Term} - \underbrace{2(\frac{\partial^2{}_{xy}\psi}{We} + a_{12}\frac{\partial^2 \psi}{\partial x^2})}$$

We analyzed the evolution of the different terms in the stress equations for various values of the Weissenberg number. We find that the relaxation coefficient behaves differently as we change the Weissenberg number.

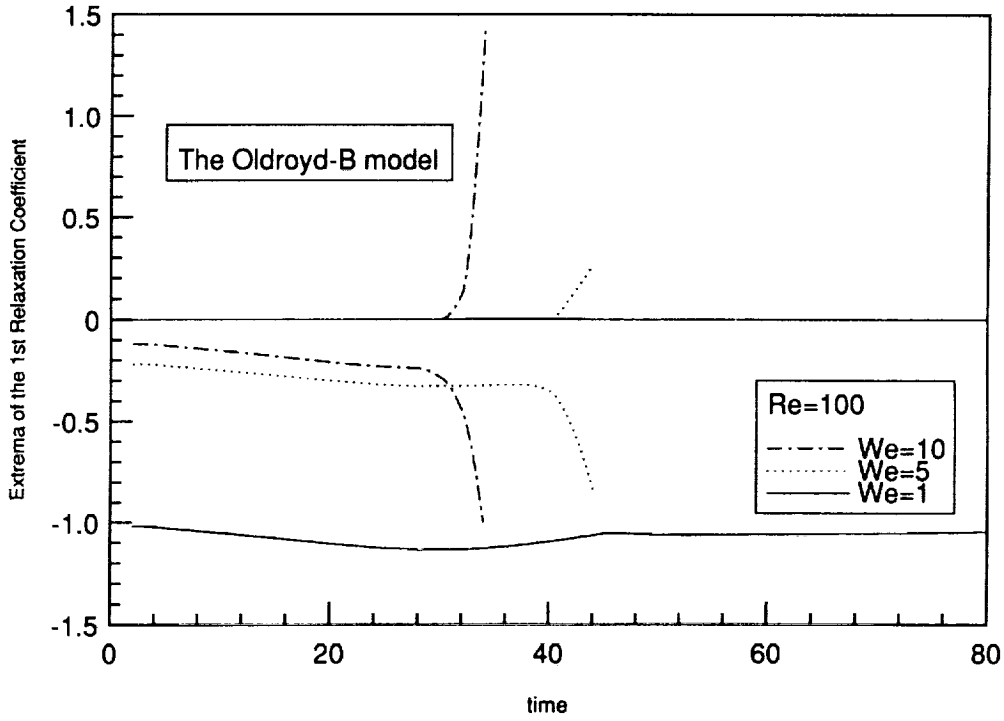

FIGURE 1. Time evolution of the first relaxation coefficient.

The "relaxation coefficients" are spatially dependent and coupled to the vorticity transport equation. Fig. 1 shows the evolution of the minimum and the maximum of the first relaxation coefficient for three different values of We. The blow-up of the code is always associated with positive values of this coefficient. (It is worth mentioning that for another rheological model, the Jeffrey's corotational model, we were able to conduct successful simulations for very large value of We. In fact the relaxation coefficients for this model are all negative and equal to $\frac{-1}{We}$.)

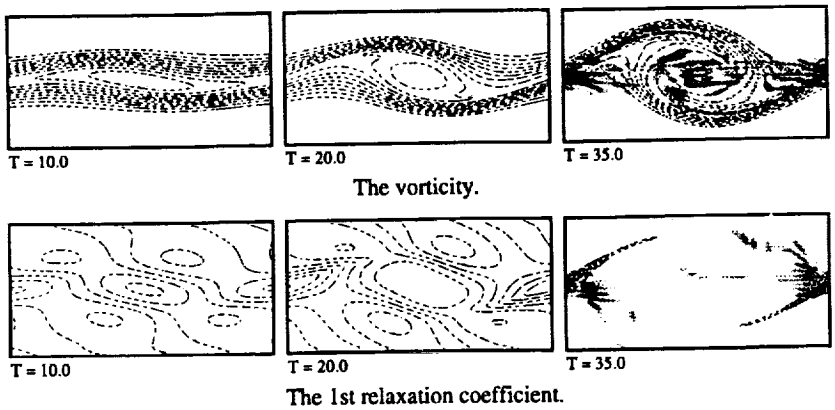

FIGURE 2. Vorticity and 1st Relaxation Coefficient Contours for the Oldroyd-B Model. Re=100,We=5.

The contour plots presented in Fig. 2 show that the regions where the first relaxation coefficient becomes positive correspond to the regions of subsequent numerical instability. In these regions, the a_{11} component of the stress tensor starts to build up, leading to a blow-up of the code. The same results are obtained for the second relaxation coefficient. As a conclusion, it resorts from this analysis that in regions of the flow where the parameter $M = We|(\frac{\partial u}{\partial x} - \frac{\partial v}{\partial y})|$ gets larger than one, the stresses start growing causing the code to blow up. The parameter M involves the elasticity of the polymer and the local normal stress in the flow.

2.3 The F.E.N.E model

The Oldroyd-B model gives a steady state elongational viscosity that goes to infinity at a finite elongational rate. This unlikely behavior results because the Hookean dumbbell model permits infinite extension. In order to avoid this unrealistic behavior, a Warner law is used instead of the Hook law leading to the FENE model. This model is described by Mackay and Petrie (1989) and the rheological equation is:

$$a_{ij}Z + We\frac{\delta a_{ij}}{\delta t} = \dot{\gamma}_{ij} + \frac{DlnZ}{Dt}(\mathbf{I} + a_{ij}We) \tag{6}$$

where $Z = 1 + \frac{n}{b}(1 + \frac{We}{n}a_{ii})$, $n = 2$ for a two dimensional flow. The FENE model is characterized with a third parameter b, related to the nature of the spring used to model the macromolecule. When $b \to \infty$ this rheological model reduces to the Oldroyd-B model. In the numerical solution of Eq. (6), $\frac{DlnZ}{Dt}$ was derived from the transport equation for a_{ii}. The finite extension properties of the FENE model allows full nonlinear simulation of roll-up.

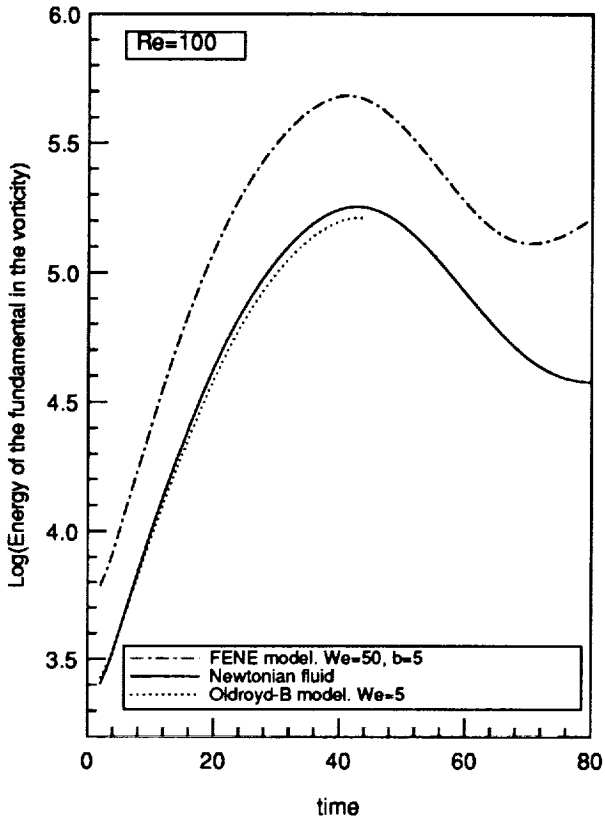

FIGURE 3. Evolution of the energy of the perturbation.

The evolution of the energy in the fundamental is presented in Fig. 3. The region of linear growth shows that the non-Newtonian mixing layer described by the FENE model is more unstable than the Newtonian mixing layer. As we shall see later, the roll-up occurs faster in the non-Newtonian case and the structure of the mixing layer changes from the Newtonian case. This higher instability of the non-Newtonian mixing layer agrees with our linear stability analysis (not discussed here).

Fig. 5 shows contour plots of the vorticity for $Re = 100, We = 50$, and $b = 5$. Notice the changes in the structures of the roll-up as compared to the Newtonian case (Fig. 4). The average value of the vorticity does not differ much from the Newtonian case, but its distribution has clearly changed. Intense accumulation of vorticity tends to occur in the braids and continue into a spiral form within the core of the vortex. The intense gradients of vorticity persist for a longer time in the core, leading to a faster and more intense roll-up.

3. Conclusion and future plans

The simulation of the non-Newtonian mixing layer was very instructive and seems

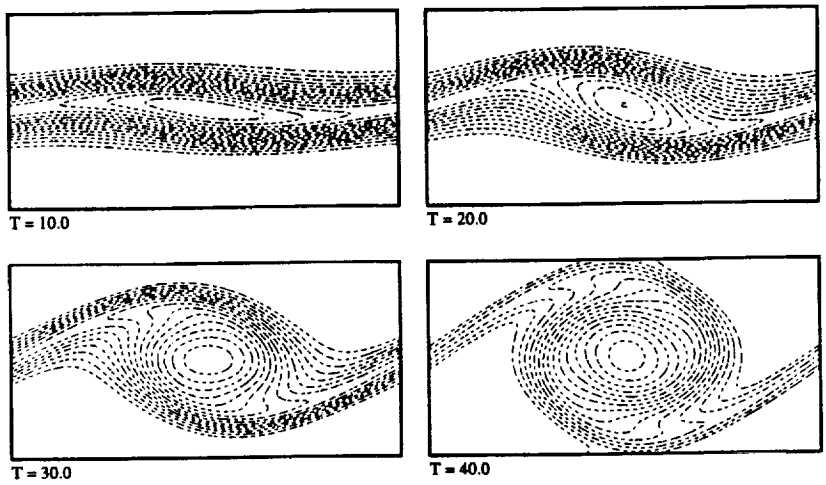

FIGURE 4. Vorticity contours for the Newtonian fluid. Re=100.

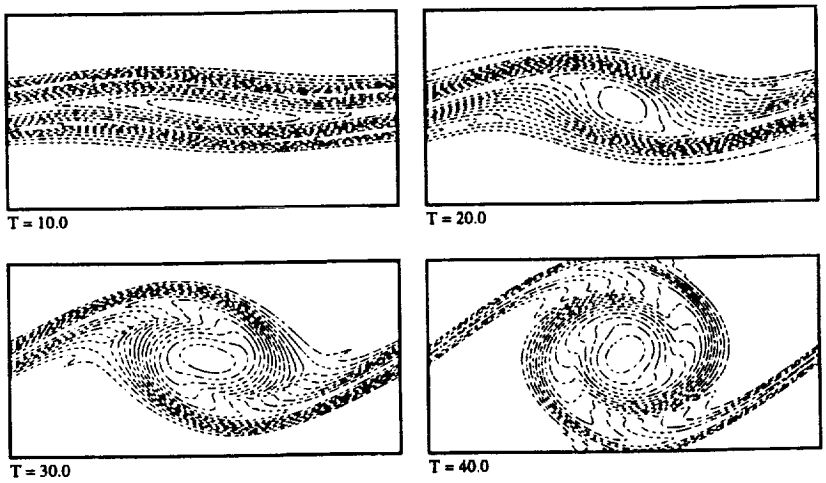

FIGURE 5. Vorticity contours for the FENE model. Re=100, We=50, and b=5.

to be very promising for reaching a better understanding of the mechanisms of instability of the mixing layer and for controlling them through polymer additives. For the Oldroyd-B rheological model, the numerical code ceases to converge whenever one of the relaxation coefficients in the stress equations becomes positive. These coefficients involve the elasticity of the polymer and the extensional stress in the flow. We propose to pursue this analysis in order to understand the physical meaning of these coefficients in terms of the coupling between viscoelastic and inertia effects.

The numerical simulations using the FENE model lead to very interesting results.

For the parameters studied, free shear flows described by this rheological model are more unstable than their Newtonian counterparts and we obtained a fairly good description of the effects of viscoelasticity on the roll-up. The process of roll-up for these flows occurs quickly and induces intense gradients of vorticity in the braids and the core of the flow. The next step of the present study is to study the effects of viscoelasticity on pairing. We will then proceed to examine the effects on vortex stretching and the streamwise vortices of the three dimensional mixing layer.

Acknowledgement

The authors would like to acknowledge useful discussions with Professor Paolo Orlandi.

REFERENCES

AZAIEZ, J., & HOMSY, G. M. 1992 Linear stability of free shear flows of viscoelastic liquids. Submitted to *J. of Fluid Mech.*

BIRD, R. B., CURTISS, C. F., ARMSTRONG, R. C. & HASSAGER, O. 1987 *Dynamics Polymeric Liquids* , vol. 2 2nd edn. Wiley-Intersciences

BOGER, D. V. 1977 A highly elastic constant-viscosity fluid. *J. Non-Newtonian Fluid Mech.* **3,** 87-91.

CROCHET, M. J. & DELVAUX, V. 1990 Numerical simulation of inertial viscoelastic flow with change of type. *I.M.A volumes in Mathematics and its Applications. Vol. 27, p47-66*

JOSEPH, D. D. 1990 *Fluid Dynamics of Viscoelastic Liquids.* Springer-Verlag

JOSEPH, D. D., RENARDY, H. & SAUT., J. C. 1985 Hyperbolicity and change of type in the flow of viscoelastic fluids. *Arch. Rationa. Mech. Anal.* **87,** 213-251

LUMLEY, J. L. 1971 Applicability of the Oldroyd constitutive equations to flow of dilute polymer solutions. *The Physics of Fluids Vol.14, 2282-2284.*

MACKAY, M. E. & BOGER, D. V. 1987 An explanation of the rheological properties of Boger fluids. *J. Non-Newtonian Fluid Mech.* **22,** 235-243.

MACKAY, M. E. & PETRIE, S. J. 1989 Estimates of apparent elongational viscosity using the fibre spinning and pure methods calculations for a FENE-P dumbbell model and comparisons with published data. *Rheological Acta.* **28,** 281-293.

SELLIN, R.H.J. & MOSES, R.T. 1989 *Drag Reduction in Fluid Flows.* Ellis Horwood-Publishers